CHEMPHYSCHEM

On the Low-Lying Excited States of *sym*-Triazine-Based Herbicides

Josep M. Oliva,[a] M. Emilia D. G. Azenha,[b] Hugh D. Burrows,[b] Rita Coimbra,[b] J. Serxio Seixas de Melo,[b] Moisés Canle L.,*[c] M. Isabel Fernández,[c] J. Arturo Santaballa,[c] and Luis Serrano-Andrés[d]

We report a joint computational and luminescence study on the low-lying excited states of sym*-triazines, namely, 1,3,5-triazine (**1**) and the ubiquitous herbicides atrazine [6-chloro-N^2-ethyl-N^4-isopropyl-1,3,5-triazine-2,4-diamine (**2**)] and ametryn [6-methylthio-N^2-ethyl-N^4-isopropyl-1,3,5-triazine-2,4-diamine (**3**)]. Geometrical structures, energetics, and transition and state properties of **1** and **2** were computed at the TD-DFT, CASSCF, and CASPT2 levels of theory. The fluorescence and phosphorescence emission spectra, lifetimes, and fluorescence quantum yields were measured for the three compounds, and from these, the energies of the lowest excited states and their corresponding radiative rates were determined. The predictions from CASPT2 calculations are in good agreement with the experimental results obtained from the luminescence studies and allow the interpretation of different absorption and emission features.*

Introduction

sym-Triazines are widely used as pest-control agents, particularly as systemic herbicides that act as photosynthesis inhibitors.[1–3] Intensive agricultural use of these compounds has led to their increasing unwanted occurrence in natural waters,[4–9] especially groundwaters.[9–11] As a consequence, public concern has grown about the long-term environmental and health effects of such pollutants.[12,13]

Many different techniques, including chlorination,[14] ozonation,[15] H_2O_2-promoted oxidation,[16] biological degradation,[17] Fenton oxidation,[18] radiolysis,[19] photocatalysis,[20] photosensitization,[21] and reduction,[22] have been attempted with questionable success to promote the degradation or elimination of these pollutants. A possible alternative is direct photodegradation, for which a number of studies on photoproducts have been performed, but little mechanistic information is available.[23–27] Proper modeling of the environmental fate of these agrochemicals will be difficult unless detailed mechanistic understanding becomes available. Indeed, a comprehensive study of the photodegradation process must involve proper knowledge of the nature and role of their different low-lying excited states.

The characteristics and properties of the excited states of azines have attracted the interest of chemists for at least 50 years. A wide variety of both theoretical (semiempirical to ab initio level) and experimental studies have been carried out on their electronic transitions.[28–39] However, there are still many unanswered questions regarding the nature of the excited states. Therefore, within the framework of a wider project aiming to elucidate the molecular mechanisms of photodegradation of different water pollutants, we report the results of a joint computational and luminescence study of the low-lying singlet and triplet states of three different *sym*-triazines (see Scheme 1), and discuss their role in the photodegradation mechanism. Fluorescence and phosphorescence emission spectra, lifetimes, and fluorescence quantum yields were measured for the three compounds, while quantum chemical calculations on the low-lying singlet and triplet excited states at different levels of theory were performed to rationalize some of the experimental findings.

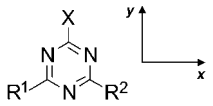

Scheme 1. *Molecular formula of the species studied in this work: 1,3,5-triazine (**1**; X = R^1 = R^2 = H), atrazine (**2**; X = Cl, R^1 = NHEt, R^2 = NHiPr), and ametryn (**3**; X = SCH$_3$, R^1 = NHEt, R^2 = NHiPr).*

[a] *Dr. J. M. Oliva*
Instituto de Química Física "Rocasolano"
Consejo Superior de Investigaciones Científicas
Serrano 119, 28006 Madrid (Spain)

[b] *Dr. M. E. D. G. Azenha, Prof. Dr. H. D. Burrows, R. Coimbra, Dr. J. S. Seixas de Melo*
Departamento de Química, Universidade de Coimbra
3004-535 Coimbra (Portugal)

[c] *Dr. M. Canle L., Dr. M. I. Fernández, Dr. J. A. Santaballa*
Departamento de Química-Física e Enxeñería Química I
Universidade da Coruña
Rúa Alejandro de la Sota, 1, 15008 A Coruña (Spain)
Fax: (+34) 981-167-065
E-mail: mcanle@udc.es

[d] *Dr. L. Serrano-Andrés*
Departamento de Química-Física e Instituto de Ciencia Molecular
Universitat de València
Dr. Moliner 50, Burjassot, 46100 Valencia (Spain)

Supporting information for this article is available on the WWW under http://www.chemphyschem.org or from the author.

  DOI: 10.1002/cphc.200400349

Experimental Procedures and Computational Details

Experimental Procedures: **1** was obtained from Aldrich and dried prior to usage. **2** and **3** were Pestanal certified standards from Riedel de Häen. All these reagents were used without further purification. Organic-matter-free freshly double distilled water was used to make up all solutions. In all cases the solutions were saturated with appropriate gases at 298.0 K and atmospheric pressure, as indicated in tables and figures.

The pH of the solutions used were those imposed by their typical macroscopic pK_1 value (approximately 5).[40,41] pH measurements were made at 298.0 K using a combined glass electrode, previously calibrated with commercial buffers of pH 7.02 $\pm$ 0.01 and pH 4.00 $\pm$ 0.01. The accuracy in the pH measurement was typically $\pm$0.02 pH units.

Spectrophotometric measurements were made on a double-beam Kontron Uvikon 941 or on a Shimadzu 2100 Plus spectrophotometer, using standard quartz cells with 10 mm path length and 3.5 mL capacity. The cells were water-flow thermostatically controlled to within $\pm$0.1 K.

Fluorescence spectra were recorded on a Jobin-Ivon SPEX Fluorog 3-22 spectrometer. All spectra were obtained in right-angle geometry and were corrected for the instrumental response of the system. Fluorescence measurements were made by using standard 1 cm^2 cross section quartz cuvettes. Fluorescence quantum yields were determined by using tryptophan[42] or bithiophene as standard.[43] Phosphorescence measurements were made by using a 1934D phosphorimeter accessory with the above instrument, with samples studied as glasses in quartz tubes of approximately 1 mm diameter cooled in liquid nitrogen in a quartz Dewar flask.

Fluorescence decays were measured with a home-built time-correlated single photon counting apparatus with an H_2-filled IBH 5000 coaxial flashlamp as excitation source, Jobin-Ivon monochromator, Philips XP2020Q photomultiplier, Canberra instruments time-to-amplitude converter, and a multichannel analyser. Alternate measurements (1000 counts per cycle), controlled by Decay® software (Biodinâmica-Portugal), of the pulse profile at 280 nm and the sample emission were performed until (1–2) $\times 10^4$ counts at the maximum were reached.[44] The fluorescence decays were analyzed by the modulating functions method of Striker et al. with automatic correction for the photomultiplier "wavelength shift".[45] Data were analyzed with ad hoc software. The reported rate constants and lifetimes were averaged over replicated experiments, with reproducibility within 5%.

Theoretical Methods and Computational Details: Geometries for the ground and excited states of **1** were optimized by computing analytical CASSCF gradients. The ground state geometry of **2** was obtained at the DFT/B3LYP level and characterized as a minimum structure. The 6-31G* basis set was finally used in all calculations. Other basis sets such as cc-pVDZ, cc-pVTZ, and aug-cc-pVDZ were also employed to calibrate the obtained results. The atom labeling and main (C–N, C–Cl) bond lengths [Å] of the computed molecules in the different optimized states are given in Scheme 2. The remaining structural details for the different states are given in the Supporting Information.

The CASSCF calculations included an active space of nine active electrons (six π plus three lone pairs) in 12 molecular orbitals. Some states were optimized with planarity restrictions. The molecule was placed in the *xy* plane (see Scheme 1 for orientation). The

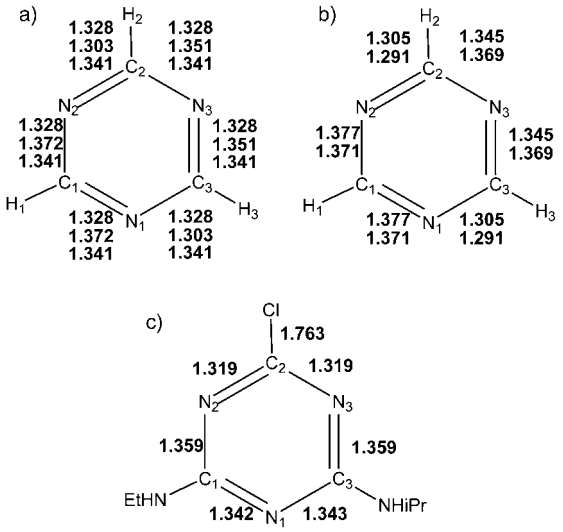

Scheme 2. *Atom labeling and main (C–N, C–Cl) bond lengths [Å] for the optimized states: a) S_0, S_1 ($^1E''_a$), and S_2 ($^1A_1''$) states for **1** (from top to bottom), b) T_1 ($^3E''_a$) and T_2 ($^3A_{22}''$) states for **1** (from top to bottom), and c) S_0 state for **2**. For the remaining parameters and structures of other states, see Supporting Information.*

ground and low-lying excited singlet states have also been found experimentally to be planar.[46,47] For the sake of simplicity, the D_{3h} symmetry found for the ground state of **1** was used to characterize its electronic states, although, upon relaxation, in some of the excited states the symmetry of the molecule reduces to C_{2v}. At the CASSCF level, five of the states maintain D_{3h} symmetry at their optimized geometries: the ground, $n\pi^*$ $^1A_1''$, $\pi\pi^*$ $^1A_2'$, $n\pi^*$ $^3A_1''$, and $\pi\pi^*$ $^3A_2'$ states. The other states reach C_{2v} optimized structures: the $n\pi^*$ $^1A_2''$, $n\pi^*$ $^1E''$ (two components, *a* and *b*), $n\pi^*$ $^3A_2''$, $n\pi^*$ $^3E''$ (two components, *a* and *b*), and $\pi\pi^*$ $^3A_2'$ states. Within the D_{3h} (C_{2v}) symmetry point groups, the states of **1** are classified as: $1^1A_1'$ (1^1A_1), $1^{1,3}E_a''$ ($1^{1,3}A_2$), $1^{1,3}A_1''$ ($2^{1,3}A_2$), $1^{1,3}A_2''$ ($1^{1,3}B_1$), and $1^{1,3}E_b''$ ($2^{1,3}B_1$). More details can be found in the Supporting Information. In **1** the labels that imply an energy ordering (e.g., S_n and T_n) are based on the computed adiabatic (T_e) ordering, and those in **2** on the computed vertical ordering.

At the different geometries of **1** and **2**, by using the multiconfigurational functions as reference, second-order perturbation theory (CASPT2 method)[28,48] was employed to obtain accurate excitation energies. The strategy of combining CASSCF geometries with CASPT2 energies (CASPT2//CASSCF protocol) has previously been shown to yield good results.[49,50] The active space employed for **2** was the same as that used for **1**. In particular for **2**, and because of its larger size, the LS-CASPT2 method[48] was used in order to include an imaginary level shift parameter of 0.2 a.u. (selected after calibration of the stability in the results), which prevents the presence of spurious intruder states in the calculation. In all cases, oscillator strengths were computed by using CASSCF transition dipole moments and CASPT2 excitation energies. In the calculation of the spontaneous emission rate for the one-photon allowed transitions, the absorption CASSCF transition dipole moments computed at the ground-state geometries and theoretical (T_e) CASPT2 (**1**) or experimental (**2**) energy differences were used.[51] No vibrational zero-point energy corrections were considered.

Calculations on the low-lying excited states of triazine computed with CI singles (CIS) and time-dependent density functional theory (TD-DFT) with the B3LYP functional were also included[52] to check

the suitability of these methods for obtaining an accurate description of the excited states in these molecules.

The calculations were performed with the MOLCAS-5[53] and Gaussian 98[52] quantum chemistry packages, and checked carefully in **1** for the convergence of the employed methods for the number of excited states included in the study. Increasing the basis sets to cc-pVDZ, cc-pVTZ, or aug-cc-pVDZ in specific cases had no significant consequences for ordering and description of the states; therefore, we decided to use the 6-31G* basis throughout. This also holds true for increases in the CAS active space. Using the B3LYP S_0 instead of the CASSCF geometry of **1** to compute the vertical spectrum changed the excitation energies by less than 0.1 eV.

Results and Discussion

Absorption and Fluorescence of Triazines

The absorption spectra of *sym*-triazines were measured in aqueous solution (Figure 1). In the case of **1**, previously reported spectra for the low-energy region in the gas phase[54–56] and in hexane[57] showed two distinctive bands up to 6 eV (207 nm): a clear medium-intensity band with a maximum at 4.59 eV (270 nm) and a very weak peak around 5.7 eV (218 nm), which in hexane has one-sixth of the intensity of the 4.59 eV peak. We also observed two absorption bands in water, blue-shifted relative to hexane or the gas phase to 206 and 260 nm, respectively, but with similar molar absorption coefficients ($\varepsilon_{206} = 993\ M^{-1}cm^{-1}$, $\varepsilon_{260} = 618\ M^{-1}cm^{-1}$). This blue shift of about 0.18 eV was previously reported for the long-wavelength band on going from *n*-hexane to water.[30] The absorption spectrum of **2** in water shows a band at 223 nm and a shoulder around 263 nm. The absorption at 223 nm ($\varepsilon_{223} = 34\,400\ M^{-1}cm^{-1}$) is considerably more intense than the shoulder ($\varepsilon_{263} = 3500\ M^{-1}cm^{-1}$) and both bands of **1**. For **3**, the spectrum in water shows two bands at 222 nm ($\varepsilon_{222} = 36\,600\ M^{-1}cm^{-1}$) and 270 nm ($\varepsilon_{270} = 3920\ M^{-1}cm^{-1}$) that follow a pattern similar to the case of **2**. Absorbance data are presented in Table 1.

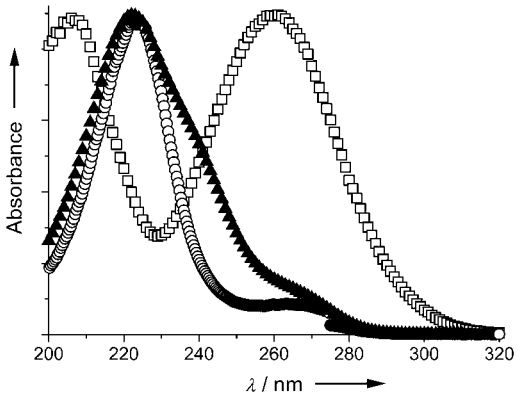

Figure 1. *UV/Vis spectra of **1** (□), **2** (○), and **3** (▲) in water. Absorbances have been normalized for the sake of comparison.*

Fluorescence spectra were obtained in aqueous solutions for **2** and **3** (Figure 2). Very weak emissions were observed, with maxima around 400–420 nm. Previous studies on **1** in the vapor phase showed a broad emission with a maximum around 400 nm,[59] while for 2,4,6-triaryl-1,3,5-triazines in acetonitrile,[60] the fluorescence maxima depend on the number and type of substituents, and vary from 414 to 460 nm. The fluorescence quantum yields Φ_F and lifetimes τ were measured in water and acetonitrile. From these, the radiative decay $k_F = \Phi_F/\tau$ and nonradiative rate constants k_{nr} can be calculated. In addition, low-temperature spectra were measured in water, ethanol/methanol, and 3-methylpentane (3MP) glasses. Solvents were chosen on the basis of solubility, while at the same time attempting to be as close to natural environments as possible. Spectral and photophysical data are presented in Table 1.

The Φ_F values are all very low. This has two consequences: first, the values have large uncertainties. Second, but more important, is that they show the importance of nonradiative

Table 1. *Absorbance maxima, molar absorption coefficients, maxima of fluorescence emission, fluorescence quantum yield, lifetimes and rate constants, maxima and lifetimes of phosphoresce emission, nonradiative decay rate constants, radiative lifetimes and SB[58] lifetimes.*

Triazine	Solvent	λ_{max} [nm]	ε [$M^{-1}cm^{-1}$]	λ_F [nm]	Φ_F	τ_F [ns]	k_F [ns^{-1}]	λ_P [nm]	τ_P [ms]	k_{nr} [ns^{-1}]	τ_{rad}^{o} [ns]	τ_{rad}^{SB} [ns]
1	H_2O	206 260	993 618	415		3.5		424	8.3			160
	CH_3CN			443								
	3MP			397	3.1×10^{-4}			428	2.7			
	EtOH/ MeOH							431				
2	H_2O	223 263	34400[25] 3500[25]	415	1.5×10^{-4}	3.2	4.7×10^{-5}	440	18	0.31	2.13×10^{4}	29
	CH_3CN			430	1.2×10^{-4}	3.0	4.0×10^{-5}			0.33	2.5×10^{4}	
	3MP			432	7.2×10^{-4}			450– 454	12.6			
	EtOH/ MeOH			405					438			
3	H_2O	222 270	36575[25] 3918[25]	405	4.7×10^{-4}	3.1	1.5×10^{-4}	430	1.9	0.32	6.7×10^{3}	26
	CH_3CN			420	1.8×10^{-4}	2.0	9.0×10^{-5}			0.50	1.1×10^{4}	
	3MP			416	5.8×10^{-4}			438	12.4			

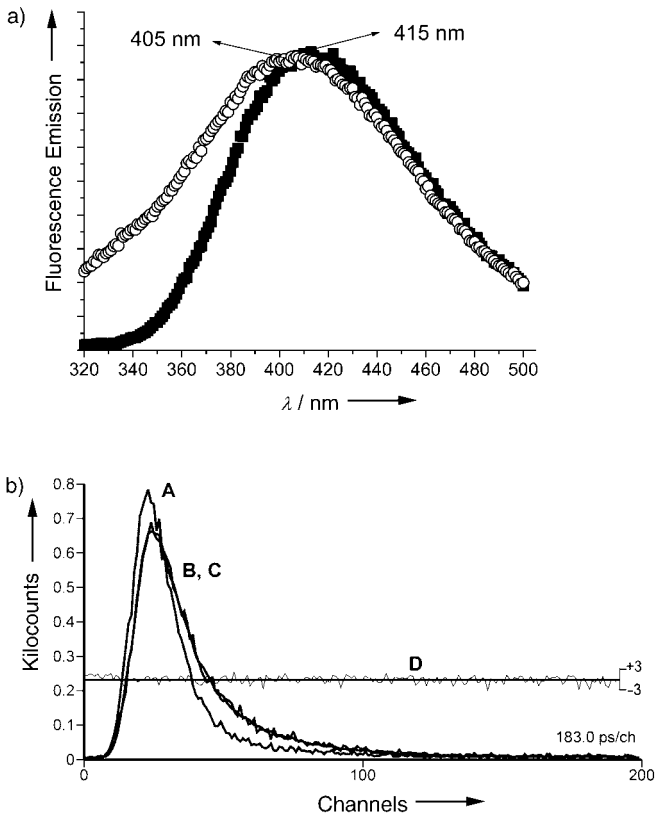

Figure 2. *a) Fluorescence emission spectra of* ***2*** *(■) and* ***3*** *(○) in N_2-saturated water at room temperature, $\lambda_{exc} = 280$ nm. Fluorescence intensities have been normalized for the sake of comparison. b) Fluorescence decay for* ***2*** *in H_2O at room temperature; curve A is the lamp pulse, B the fluorescence decay for* ***2****, C the first-order decay fit, and D the residuals of the fit.*

pathways in deactivation of the lowest excited singlet state of triazines. Furthermore, differences of orders of magnitude were observed in the natural radiative lifetimes of the lowest excited singlet state obtained from the experimental radiative decay constants ($\tau_{rad} = 1/k_f$) and the values calculated (Table 1) from molar absorption coefficients by using the Strickler–Berg (SB) approach.[58] For example, for **2** in water the values are about 2.1×10^4 ns from quantum yield and lifetime, and 29 ns from SB. This strongly suggests that the lowest energy band observed in the absorption spectrum is not that responsible for the fluorescence. This data is compatible with an allowed visible transition for the three triazines at about 260–270 nm (4.6–4.8 ev), probably of $n\pi^*$ character in **1** (although with noticeable oscillator strength) and of $\pi\pi^*$ character in **2** and **3**, whilst the emission originates from a lowest $n\pi^*$ state of forbidden character, whose absorption band is buried under the tail of the allowed transition. Theoretical calculations support these conclusions (see below).

The nonradiative decay of S_1 involves both internal conversion and intersystem crossing. Although, in principle, direct observation of the triazine triplet–triplet absorption by flash photolysis would allow determination of the yield of intersystem crossing, and such an absorption has been reported for 1,3,5-triazine in acetonitrile solution,[38] we have not yet been able to obtain reliable triplet absorption data for these three triazines. Work is in progress on this.

Table 2 compiles the calculated absorption and emission energies and transition and state properties for the low-energy singlet states of **1** at different levels of theory. In the following discussion, only CASPT2 energies are considered, as they represent the best available theoretical data. Other results are compared later. Table 3 combines the compared experimental data of Table 1 and the theoretical results obtained for **1**, as well as the assignments performed, based on both experimental and theoretical evidence. For **1**, the enumerative labels (S_n, T_n) follow the order established by T_e at the CASPT2 level.

Our interest was first focused on the lowest energy region of the absorption spectrum and on the fluorescence spectrum. Regarding the absorption bands, transitions computed at the ground-state optimal geometry can be approximately related

Table 2. *Computed CI singles (CIS), TD-DFT/B3LYP (B3L), CASSCF (CAS), and CASPT2 (PT2) energy differences and transition and state properties for the low-lying excited singlet and triplet states of* ***1****.*

State[d]	E_{VA}[a] [eV] CIS	B3L	CAS	PT2	f[e]	T_e[b] [eV] CAS	PT2	E_{VE}[c] [eV] PT2	μ[f] [D]	τ [ns]
$^1A_1'$, S_0									0.00	
$^1A_1''$, $n\pi^*$, S_2	6.73	4.51	5.90	4.11	–	5.61	3.89	3.38	0.00	–
$^1A_2''$, $n\pi^*$, S_4	6.39[g]	4.61[g]	5.11	4.30	0.027	4.59	4.09	3.60	2.02	53[h]
$^1E''_a$, $n\pi^*$, S_1	6.53	4.60	5.51	4.32	–	4.85	3.69	2.71	1.65	–
$^1E''_b$, $n\pi^*$, S_3	6.53	4.60	5.51	4.32	-	5.23	4.08	3.76	0.12	–
$^1A_2'$, $\pi\pi^*$, S_5	7.18	6.25	5.55	5.59	–	5.25	5.17	5.07	0.00	–
$^3A_{22}''$, $n\pi^*$, T_2	5.45	3.92	4.63	3.87	–	4.20	3.69	3.07	2.09	–
$^3E''_a$, $n\pi^*$, T_1	5.74	4.13	5.13	4.04	–	4.53	3.54	2.67	1.24	–
$^3E''_b$, $n\pi^*$, T_3	5.74	4.13	5.13	4.04	–	4.81	3.77	3.46	0.17	–
$^3A_{21}''$, $n\pi^*$, T_4	6.52	4.38	5.92	4.15	–	5.59	3.95	3.65	0.00	–
$^3A_{22}'$, $\pi\pi^*$, T_5	4.25	4.40	4.34	4.76	–	4.10	4.39	4.31	0.00	–

[a] Vertical excitation: calculations at the ground state (S_0) with optimized CAS geometry. [b] Band origin: energy difference between S_0 and the corresponding excited state at their respective optimized CAS geometries. [c] Vertical emission: energy difference between the excited and ground states at the optimized CAS geometry of the corresponding excited state. [d] The enumerative labels (S_n) follow the order established by T_e (CASPT2). [e] Oscillator strength obtained by using the CAS transition dipole moment and the PT2 (E_{VA}) energy. [f] CAS dipole moment at the excited state CAS optimized geometry (all zero at the S_0 D_{3h} geometry). [g] Oscillator strengths computed as 0.034 and 0.015 at the CIS and B3L levels, respectively.[51,58] [h] Estimated by using the Strickler–Berg (SB) equation.

Table 3. *Theoretical (CASPT2) and experimental transitions in the spectra of* ***1****. Assignments based both on theoretical and experimental grounds.*

State	Absorption maxima [eV] ([nm]) Theory	Experiment	Band origins [eV] ([nm]) Theory	Experiment	Emission maxima [eV] ([nm]) Theory	Experiment
$^3E''_a$			3.54	3.59 (345)[a]	> 2.67	2.93 (423)[c]
$n\pi^*$, T_1				3.4–3.3 (365–376)[b]		2.88 (430)[c]
$^1E''_a$			3.69	3.83 (324)[d–f]	> 2.71	2.99 (415)[g]
$n\pi^*$, S_1						2.8 (443)[g]
$^1A_2''$	4.30	4.59 (270)[h]	4.09	4.02 (308)[j]		
$n\pi^*$, S_4		4.77 (260)[i]				
$^1A_2'$	5.59	5.7 (218)[k]				
$\pi\pi^*$, S_5		6.0 (206)[l]				

[a] Gas-phase spectrum. Suggested as excited vibrational band of the $^3E''$ state.[61] [b] From the estimated S–T splitting in the laser-induced fluorescence of **1** in a matrix.[62] [c] Phosphorescence maxima in water and 3MP, respectively (this work). [d] Two-photon photoacoustically detected gas-phase spectrum.[47] [e] Optical spectrum in the vapor phase.[60] [f] Laser-excited fluorescence in vapor of **1**.[63] [g] Fluorescence maxima in H_2O and CH_3CN ($\lambda_{exc} = 270$ nm), respectively (this work). [h] Weak band maxima in the gas phase[54–56] and hexane.[57] The experimental[54] and theoretical oscillator strengths are 0.013 and 0.027, respectively. [i] Absorption maxima in water (this work). [j] Estimated $^1A_2''$ origin in the two-photon photoacoustically detected gas-phase spectrum.[47] [k] Weak peak in the gas phase[54–56] and hexane[57] spectra. In hexane it has one-sixth the height of the 4.56 eV peak.

to the band maxima in the gas phase. The four low-lying singlet excited states at this geometry are of $n\pi^*$ character. The one-photon forbidden $^1A_1''$ $n\pi^*$ state is found to be vertically the lowest singlet excited state at 4.11 eV. About 0.2 eV above this, two other $n\pi^*$ states are computed: the one-photon allowed $^1A_2''$ state at 4.30 eV and the doubly degenerate one-photon forbidden, two-photon allowed $^1E''$ state at 4.32 eV. The low-lying $\pi\pi^*$ transition is computed to be related to a dipole-forbidden $^1A_2'$ state at 5.59 eV. The results obtained are in agreement with previous CASPT2 data reported for triazine,[28] and can be compared with the measured absorption spectra. The band maximum recorded in the gas phase at 4.56 eV[54–56] with estimated values for the oscillator strength of 0.013[54] or 0.0210[30] is therefore attributed to the one-photon allowed transition to the $^1A_2''$ $n\pi^*$ state, computed to be at 4.30 eV, with a calculated oscillator strength of 0.027. The weak feature observed at 5.7 eV[54,56] can be assigned as corresponding to excitation to the one-photon forbidden $^1A_2'$ $\pi\pi^*$ state. The peak reported at 3.97 eV (312 nm)[54,64] has been previously assigned to the 6_0^1 vibrational excitation of the $^1E''$ state.

Different band origins have been assigned from experimental studies. There is strong evidence that the $^1E''$ state, located in the vapor phase at 3.83 eV (324 nm),[47,55,63] yields the lowest-lying singlet–singlet absorption from the ground state. The theoretical data support this conclusion. The CASPT2//CASSCF results place the $^1E''$ band origin (T_e) at 3.69 eV, 0.2 eV below any other singlet excited state. Therefore, this state can be considered to be the lowest singlet excited S_1 state. Note, however, that the geometry optimization led to splitting of the two components of the D_{3h} $^1E''$ state into two different C_{2v} excited states. The component labeled *a* becomes adiabatically the first singlet state of $^1A_2$ (C_{2v}) symmetry, while the *b* component becomes the second singlet state of $^1B_1$ symmetry. Webb et al.[47] estimated the T_0 transition to the one-photon allowed $^1A_2''$ state to be 0.19 eV above the $^1E''$ origin, that is, at 4.02 eV (302 nm). This is in fair agreement with our calculation for the band origin (T_e) of this state at 4.09 eV. Because of the congestion and complexity of the spectrum, further assignments based on the theoretical results cannot be obtained. The accuracy of the calculations is expected to be within 0.1–0.2 eV. The computations predict the occurrence of the $^1A_1''$ bands in the low-lying spectrum, starting from a band origin at 3.89 eV. This state has not been found experimentally, although there is evidence of its presence.[47]

The fluorescence spectra reported here for **1** in water display a band maximum at 2.99 eV (415 nm). On the basis of the vertical emission computed at 2.67 eV (which can be considered as a lower bound for the emission maxima), and the previous arguments on the basis of experimental radiative lifetimes, we can assign the fluorescence as originating from the $^1E''$ $n\pi^*$ state. This is expected on the basis of Kasha's rule[65] that radiative processes always take place from the lowest electronic state of a given spin multiplicity, independent of the energy of the electronic state to which the species was initially excited. Only the transition to the $^1A_2''$ state is one-photon allowed in the low-lying spectrum, and we can estimate from theory the SB radiative lifetime of the $^1A_2''$ state to be 53 ns. In water, and based on the lowest energy absorption band, the SB radiative lifetime of **1** was estimated to be 160 ns. Considering that a state different from that related to the lowest one-photon allowed band in absorption (S_4, $^1A_2''$, $n\pi^*$) is computed to be the fluorescing state, S_1 ($^1E''$) $n\pi^*$, the measured radiative lifetime can be expected to be several orders of magnitude larger. From the experimental fluorescence decay time in water, and assuming a similar fluorescence quantum yield to those of **2** and **3** in this solvent, an experimental lifetime of about 3×10^4 ns can be estimated.

For the much larger molecule of **2**, only vertical calculations at the ground-state geometry were performed at the different levels of theory. The results are compiled in Table 4. Unlike **1**, the enumerative labels (S_n, T_n) follow the order established by the vertical (not the adiabatic) calculations at the CASPT2 level. The structure and appearance of the low-lying absorption spectrum of **2** are significantly different to those of **1**. Two absorption bands are observed in water, with maxima at 4.71 eV (263 nm) and 5.56 eV (223 nm). The positions of the bands are very similar to those observed for **1** in the vapor phase (4.59 and 5.70 eV), but this is just a coincidence that may lead to confusion. In atrazine the low-energy band is much weaker than the 5.56 eV band. The analysis of the theoretical spectrum confirms that the ordering of excited states has changed with respect to **1** at the ground-state geometry. Vertically, the lowest excited singlet state of **2** has $\pi\pi^*$ character and is com-

Table 4. *Computed CI singles (CIS), TD-DFT/B3LYP (B3L), CASPT2 (PT2) energy differences [eV], oscillator strengths f, dipole moments μ (CASSCF), and radiative lifetimes for the low-lying excited singlet and triplet states of* ***2****. Recorded band maxima in water.*

State	CIS	*f*	B3L	*f*	PT2	*f*	μ [D]	τ[a] [ns]	Absorption maxima [eV] ([nm])
S_0							4.16		
S_1 ($\pi\pi^*$)	6.92	0.176	5.15	0.032	4.89	0.025	4.44	170	4.71 (263)[e]
S_2 ($n\pi^*$)[b]	7.56	0.011	5.43	0.005	5.06	0.001	3.45	4363	
S_3 ($n\pi^*$)[b]	7.30	0.000	5.28[c]	0.001	5.22	0.001	2.81	4500	
S_4 ($\pi\pi^*$)	7.75	0.030	5.46[c]	0.002	5.37	0.157	7.16	30	
S_5 ($n\pi^*$)[b]	8.21	0.000	5.98	0.000	5.54	0.025	2.02		5.56 (223)[e]
S_6 ($\pi\pi^*$)	8.49	0.449	6.24	0.147	5.79	0.153	5.44		
S_7 ($n\pi^*$)[b]	8.63	0.034	6.04	0.150	5.95	0.050	3.01		
S_8 ($\pi\pi^*$)	7.93	1.319	6.27	0.791	6.05	0.667	4.97		
T_1 ($\pi\pi^*$)	5.35	–	4.27	–	4.81	–	4.67		
T_2 ($\pi\pi^*$)	5.39	–	4.32	–	4.85	–	3.94		
T_3 ($n\pi^*$)[d]	6.98	–	5.04	–	5.05	–	3.39		
T_4 ($n\pi^*$)[d]	6.75	–	5.02	–	5.12	–	5.54		
T_5 ($\pi\pi^*$)	6.61	–	4.93	–	5.33	–	3.34		
T_6 ($n\pi^*$)[d]	7.94	–	5.77	–	5.56	–	4.11		
T_7 ($n\pi^*$)[d]	7.89	–	5.72	–	5.70	–	1.51		
T_8 ($\pi\pi^*$)	6.66		5.05		5.85		6.14		

[a] Radiative lifetime computed by using the Strickler–Berg approach[51,58] and the experimental emission (415 nm). [b] The correspondence to **1** $n\pi^*$ states is: S_2 ($^1E''_a$), S_3 ($^1E''_b$), S_5 ($^1A_1''$), and S_7 ($^1A_2''$). [c] Both states have mixed $n\pi^*$ and $\pi\pi^*$ character at the B3LYP level. [d] The correspondence to **1** $n\pi^*$ states is: T_3 ($^3E''_b$), T_4 ($^3E''_a$), T_6 ($^3A_{21}''$), and T_7 ($^3A_{22}''$). [e] Extinction coefficients in water: 3500 and 34400 $M^{-1}cm^{-1}$, respectively (this work).

puted to lie at 4.89 eV with an oscillator strength of 0.025. Four other $n\pi^*$ and three $\pi\pi^*$ excited singlet states are suggested to be located at energies up to 6.1 eV. The largest oscillator strengths correspond to the $\pi\pi^*$ transitions to S_4 (0.157), S_6 (0.153), and S_8 (0.667). While the S_1 ($\pi\pi^*$) state, computed to be at 4.89 eV, can be related to the weak band observed in the absorption spectrum in water at 4.71 eV (263 nm), the 5.56 eV (223 nm) band seems to be formed by the superposition of at least two $\pi\pi^*$ transitions to the S_4 and S_6 states. The difference in dipole moments for the two states leads one to think that the gas-phase spectrum may exhibit two well-resolved bands in this region. A more intense $\pi\pi^*$ transition is predicted to the S_8 state lying slightly above 6.0 eV. With respect to the $n\pi^*$ states, the analysis of their wave functions can help us establish a correspondence with the D_{3h} states of triazine: $^1E''_a$, $^1E''_b$, $^1A_1''$, and $^1A_2''$ (see Table 4). Comparing **1** and **2**, the general trends observed in the latter are that, for the singlet excited states, there is a stabilization of the $\pi\pi^*$ states (near 0.7 eV for the low-lying state) and destabilization of the $n\pi^*$ states (0.8–1.6 eV).

Using the Strickler–Berg approach and the observed emission band at 2.99 eV (415 nm), we estimated the radiative lifetimes of the four low-lying excited states of **2** to be 170, 4363, 4500, and 30 ns, respectively, for the emissions from the states labeled S_1 to S_4 in Table 4. These values may help us to predict the nature of the fluorescing state. From the recorded fluorescence quantum yields and lifetimes in Table 1, the experimentally estimated radiative fluorescence lifetime of **2** in water is 21300 ns. This value would be more consistent with the $n\pi^*$ S_2 and S_3 states than with the $\pi\pi^*$ states. One may then speculate that the fluorescing state (the true S_1) in **2** has an $n\pi^*$ nature, as occurs in **1**, while a similar conclusion can be reached for **3**, given the resemblance of their spectra.

Phosphorescence of Triazines

Attempts were made to observe the phosphorescence of **1**, **2**, and **3** in a variety of solvent glasses at 77 K. For **1** in 50% EtOH/MeOH glass, a broad emission was observed, with a maximum around 431 nm (2.88 eV), while in water it was at 424 nm (2.93 eV) and in 3MP at 428 nm (2.90 eV). Phosphorescence decay in all three solvents could be fitted by a single exponential, and lifetimes of a few milliseconds were observed. Phosphorescence for this compound has previously been reported in an EPA (2 ethanol, 5 *i*-pentane, 5 Et_2O) glass, and shown to have a maximum around 455 nm and lifetime 0.44 s.[29] At present, the reason for the difference in lifetimes in this work and in our previous studies is not clear. Phosphorescence has also been observed for **2** and **3** in 3MP glasses at 77 K. The spectrum for **2** (Figure 3) shows a broad band with maximum at 450 nm (2.76 eV). The phosphorescence decay is

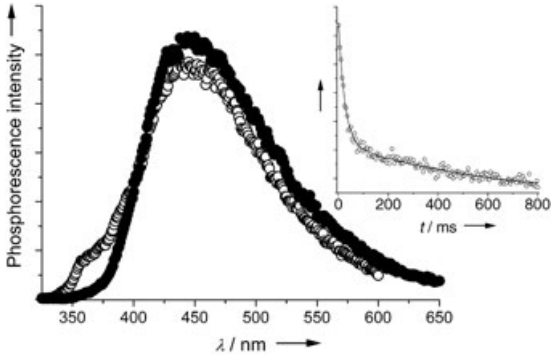

Figure 3. *Phosphorescence emission spectra of* ***2*** *(○) in 3MP at 77 K. λ_{exc} = 262 nm (○), 280 nm (●). Inset: phosphorescence decay.*

monoexponential with a lifetime of 12.6 ms. Phosphorescence data for **1**–**3** are summarized in Table 1. The phosphorescence lifetimes are intermediate between those expected for lowest lying $n\pi^*$ and $\pi\pi^*$ triplet states, and do not permit state assignment.

Theoretical calculations were also carried out on the triplet excited states, and data are given in Tables 2–4. For the triplet states of **1**, the computed CASPT2 results place four excited $n\pi^*$ states vertically below the lowest $\pi\pi^*$ $^3A_2'$ state at 4.76 eV. The lowest lying excited triplet state is computed vertically to be the $n\pi^*$ $^3A_{22}''$ state at 3.87 eV, while the $^3E''$ and $^3A_{21}''$ excited states are obtained at 4.04 and 4.15 eV, respectively. The onset of 1,3,5-triazine phosphorescence is around 3.54 eV (350 nm). Also, an absorption band reported at 3.59 eV (345 nm) has been suggested to be related to T_1,[61] while Haag et al.[62] predicted the presence of the triplet band origin near 3.3–3.4 eV (365–376 nm). This state was suggested to be of $^3E''$ character. The present theoretical results support this assignment. The lowest energy band origin is computed to correspond to the *a* component of the $^3E''$ state (1^3A_{22} in C_{2v} symmetry) at 3.54 eV, close to the experimental observation. Experimentally, the singlet–triplet (S–T) splitting has been estimated to be 0.24 eV in the spectrum of triazine in the crystal,[61] and 0.5 eV in an argon matrix.[62] Considering the band origins, our theoretical S–T splitting is 0.15 eV. The four low-lying $n\pi^*$ triplet states were computed to have band origins within a range of 0.4 eV, so that major congestion of the triplet spectra can be expected. Evidence for singlet–triplet coupling in the $^1E''$ fluorescence involving at least two different triplet states has been found.[64,66] The most effective coupling can be expected with the $^3A_{22}'$ $\pi\pi^*$ state. The presence of its band origin computed at 4.39 eV, close to the vertical excitation to the $^1E''$ state (4.32 eV), might justify the suggested coupling of the two states.[59] As for the triplet states, adiabatically it is the *a* component of the $^3E''$ state which is the lowest lying triplet state, with a computed vertical emission to the ground state at 2.67 eV, while the other states remain at least 0.4 eV higher in energy. The $^3E''$ $n\pi^*$ state (symmetry broken to $^3A_{22}$ in C_{2v}) is therefore likely to be responsible for the observed phosphorescence. The experimental phosphorescence lifetimes are consistent with emission from an $n\pi^*$ state, although they do not allow an unambiguous assignment.

For the triplet excited states of **2**, the stabilization of the $\pi\pi^*$ with respect to the $n\pi^*$ states is not as large as in **1**, and therefore the S–T splitting for the low-lying $\pi\pi^*$ state is drastically reduced on going from **1** to **2**, from 0.83 to 0.04 eV, respectively. Considerable coupling is suggested between $n\pi^*$ and $\pi\pi^*$ states and leads to a dramatic reduction in the S–T energy gap, as represented schematically in the Jablonski diagram of Figure 4. This is expected to lead to efficient intersystem crossing, which may explain the high nonradiative rates obtained from the fluorescence data and the low fluorescent quantum yields observed for these compounds. On the other hand, the $n\pi^*$ states undergo a destabilization by more than 1 eV.

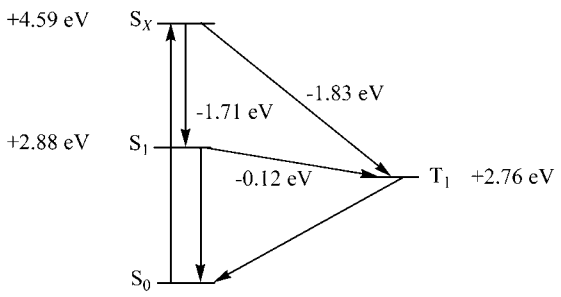

Figure 4. *Schematic Jablonski diagram for* ***2****.*

Comparison of Theoretical Methods

The results in Tables 2–4 allow us to comment briefly on the performance of the different theoretical methodologies employed. The CASPT2//CASSCF approach has become a robust computational approach for studying excited states,[48] and therefore we can use the CASPT2 results to calibrate, in particular, the TD-DFT/B3LYP (TD) data. The B3LYP functional was selected as the most general and widely used approach in the literature. The CIS results are known to be of low quality due to an unbalanced treatment of electron correlation energy included in this approach. Both the state ordering and the absolute energies are clearly erroneous, with deviations ranging from 0.5 to 2.6 eV in the two molecules. Oscillator strengths in **2** are also quantitatively incorrect. The CASSCF results, including only nondynamical correlation effects and forming the zeroth-order reference for CASPT2, may help to understand the performance of the CIS approach. The TD energies and oscillator strengths are closer to the CASPT2 results. The energy ordering of the states is practically the same in **1** for the two methods, although TD theory overestimates the CASPT2 energies by 0.3–0.7 eV. In particular, the experimental $\pi\pi^*$ absorption is overestimated by 0.55 eV at the TD level. In some cases the CASPT2 excitation energies may slightly underestimate the correct values, but in general it is well known that the energies for the singlet excited states are usually overestimated by TD-DFT approaches.[67] The situation seems to be different for the triplet states.

Unlike **1**, in **2** the TD values underestimate the CASPT2 values, and the computational problems are more serious. he TD/B3LYP method seems to be unable to deal with the mixture of states (see Table 4), and this may affect especially the calculation of the oscillator strengths, although different behavior is possible for other functionals.[68] No TD band is computed below 6.0 eV that may be assigned to the intense 5.58 eV experimental transition.

Conclusions

The lowest excited singlet and triplet states of three *sym*-triazines have been studied experimentally by absorption, fluorescence, and phosphorescence spectroscopy and lifetime measurements, and have been analyzed theoretically by various approaches. High-level results, obtained by using the CASPT2 method, allowed elucidation of the different absorption and emission features. The main absorption bands have been clear-

ly assigned in **1** and **2**. Four low-lying $n\pi^*$ singlet transitions have been identified in the absorption spectrum of **1** below the lowest $\pi\pi^*$ singlet transition, and the same structure is found for the triplet states. The low-lying emissions of **1** are assigned to the $^1E''$ $n\pi^*$ state (fluorescence) and the $^3E''$ $n\pi^*$ state (phosphorescence), which become S_1 and T_1, respectively, on decreasing their symmetry to C_{2v}. In **2**, a $\pi\pi^*$ transition is proposed to be the lowest vertical absorption, both in the singlet and triplet spectra. Considerable coupling is suggested between close-lying $n\pi^*$ and $\pi\pi^*$ states, while a dramatic decrease in the S–T energy gap relative to **1** increases intersystem crossing and therefore reduces the fluorescence quantum yield. An $n\pi^*$ state is also suggested to be the fluorescing state in **2** and **3** on the basis on the computed and observed energies and lifetimes.

Acknowledgements

Part of this work is contained in the PhD Thesis of M.I.F. (Spain) and the MSc Thesis of R.C. (Portugal). This research was carried out with financial support from projects PPQ2000-0449-C02-01 (MCyT, Spain), BQU2001-2926 (MCyT, Spain), and PGIDTO2-TAM10301PR and laboratory equipment infrastructure (XuGa, Spain), as well as through the Acciones Integradas bilateral program HP1999–0078 of the MCyT (Spain) and Conselho de Reitores (Portugal). M.E.D.G.A., H.D.B., R.C., and J.S.deM. also acknowledge financial support from FCT, FEDER, POCTI, and JMO from project BQU2003-05827 (MCyT, Spain). Research visits of M.I.F., H.D.B., and J.M.O. were funded by the Xunta de Galicia and the Universidade da Coruña.

Keywords: ab initio calculations · fluorescence · herbicides · luminescence · triazines

[1] R. T. Meister, C. Sine, *Farm Chemicals Handbook*, Meister Publishing Co., Willoughby, OH, **1998**.
[2] R. C. Worthing, *The Pesticide Manual*, *9th ed.*, British Crop Protection Council, Surrey, UK, **1991**.
[3] T. Roberts, D. H. Hutson, P. W. Lee, P. H. Nicholls, J. R. Plimmer, *Metabolic Pathways of Agrochemicals. Part 1: Herbicides and Plant-Growth Regulators*, *Vol.* 1 (Ed.: T. R. Roberts), The Royal Society of Chemistry, Cambridge, **1998**, p. 849.
[4] R. Spear in *Handbook of Pesticide Toxicology*, *Vol.* 1 (Eds.: W. J. Hayes, E. R. Laws), Academic Press, San Diego, **1991**.
[5] C. J. Miles, *Pesticide Transformation Products. Fate and Significance in the Environment*, *Vol.* 459 (Eds.: L. Somasundaram, J. R. Coats), American Chemical Society, Washington DC, **1991**.
[6] D. A. Belluck, S. L. Benjamin, T. Dawson, *Pesticide Transformation Products. Fate and Significance in the Environment*, *Vol.* 459 (Eds.: L. Somasundaram, J. R. Coats), American Chemical Society, Washington DC, **1991**.
[7] G. W. Aherne in *Chemistry, Agriculture and the Environment*, Royal Society of Chemistry, London, **1991**.
[8] E. Funari, P. Bottoni, G. Giuliano, *Chemistry, Agriculture and the Environment*, Royal Society of Chemistry, London, **1991**.
[9] K. Verschueren, *Handbook of Environmental Data on Organic Chemicals, 3rd Ed.*, Van Nostrand Reinhold, New York, **1996**.
[10] S. Galassi, L. Guzzella, *Acqua & Aria* **1990**, *3*, 231.
[11] W. D. Hörmann, J. C. Tournayre, H. Egli, *Pestic. Monit. J.* **1979**, *13*, 128.
[12] E. Hodgson, P. E. Levi, *Environ. Health Perspect.* **1996**, *104*, 97.
[13] V. Drevenkar, S. Fingler, Z. Fröbe in *Chemical Safety International Reference Manual* (Ed.: M. Richardson), VCH, Weinheim, **1994**.
[14] A. López, G. Mascolo, G. Tiravanti, R. Passino, *Water Sci. Technol.* **1997**, *35*, 129.
[15] G. Mascolo, A. López, H. James, M. Fielding, *Wat. Res.* **2001**, *35*, 1695.
[16] E. Evgenidou, K. Fytianos, *J. Agric. Food Chem.* **2002**, *50*, 6423.
[17] M. C. Bonnet, B. Welte, A. Montiel, M. Dore, *Environ. Technol.* **1991**, *12*, 217.
[18] K. H. Chan, W. Chu, *Chemosphere* **2003**, *51*, 305.
[19] G. Angelini, R. Bucci, F. Carnevaletti, M. Colosimo, *Radiat. Phys. Chem.* **2000**, *59*, 303.
[20] I. K. Konstantinou, T. M. Sakellarides, V. A. Sakkas, T. A. Albanis, *Environ. Sci. Technol.* **2001**, *35*, 398.
[21] H. Cui, H.-M. Hwang, K. Zeng, H. Glover, H. Yu, Y. Liu, *Chemosphere* **2002**, *47*, 991.
[22] A. Ghauch, J. Suptil, *Chemosphere* **2000**, *41*, 1835.
[23] M. Canle L. , M. I. Fernández, J. A. Santaballa, *J. Phys. Org. Chem.*, **2005**, *18*, 148.
[24] M. E. D. G. Azenha, H. D. Burrows, M. Canle L. , R. Coimbra, M. I. Fernández, M. V. García, A. E. Rodrígues, J. A. Santaballa, S. Steenken, *Chem. Commun.* **2003**, 112.
[25] M. E. D. G. Azenha, H. D. Burrows, M. C. L. , R. Coimbra, M. I. Fernández, M. V. García, M. A. Peiteado, J. A. Santaballa, *J. Phys. Org. Chem.* **2003**, *16*, 498.
[26] H. Burrows, M. Canle L. , J. A. Santaballa, *J. Photochem. Photobiol. B* **2002**, *67*, 71.
[27] M. I. Fernández Pérez, PhD Thesis, Universidade da Coruña (A Coruña), **2002**.
[28] M. P. Fulscher, K. Andersson, B. O. Roos, *J. Phys. Chem.* **1992**, *96*, 9204.
[29] J. P. Paris, R. C. Hirt, R. G. Schmitt, *J. Chem. Phys.* **1961**, *34*, 1851.
[30] S. F. Mason, *J. Chem. Soc.* **1959**, 1240.
[31] J. S. Brinen, J. G. Koren, W. G. Hodgson, *J. Chem. Phys.* **1966**, *44*, 3095.
[32] R. M. Hochstrasser, A. H. Zewail, *J. Chem. Phys.* **1971**, *55*, 5291.
[33] R. C. Hirt, F. Halverson, R. G. Schmidt, *J. Chem. Phys.* **1954**, *22*, 1148.
[34] J. E. Lancaster, N. B. Colthup, *J. Chem. Phys.* **1954**, *22*, 1149.
[35] K. K. Innes, J. P. Byrne, R. I. G. , *J. Mol. Spectrosc.* **1967**, *22*, 125.
[36] L. Goodman, R. W. Harrell, *J. Chem. Phys.* **1959**, *30*, 1131.
[37] L. Goodman, *J. Mol. Spectrosc.* **1961**, *6*, 109.
[38] D. V. Bent, E. Hayon, *Chem. Phys. Lett.* **1975**, *31*, 325.
[39] B. E. Pape, M. J. Zabik, *J. Agric. Food Chem.* **1970**, *18*, 202.
[40] P. Schmitt, T. Poiger, R. Simon, D. Freitag, A. Kettrup, A. W. Garrison, *Anal. Chem.* **1997**, *69*, 2559.
[41] D. R. Lide, *CRC Handbook of Chemistry and Physics: A Ready-Reference Book of Chemical and Physical Data*, CRC Press Inc., Boca Ratón, FL, **2000**.
[42] A. Tine, J. J. Aaron, *Can. J. Spectrosc.* **1984**, *29*, 121.
[43] R. S. Becker, J. Seixas de Melo, A. L. Maçanita, F. Elisei, *J. Phys. Chem. B* **1996**, *100*, 18683.
[44] J. S. Seixas de Melo, P. F. Fernandes, *J. Mol. Struct.* **2002**, *565/566*, 69.
[45] G. Striker, V. Subramaniam, C. A. M. Seidel, A. Volkmer, *J. Phys. Chem. B* **1999**, *103*, 8612.
[46] Y. Udagawa, M. Ito, S. Nagakura, *J. Mol. Spectrosc.* **1971**, *39*, 400.
[47] J. D. Webb, K. M. Swift, E. R. Bernstein, *J. Chem. Phys.* **1980**, *73*, 4891.
[48] a) K. Andersson, P.-Å. Malmqvist, B. O. Roos, *J. Chem. Phys.* **1992**, *96*, 1218; b) B. O. Roos, K. Andersson, M. P. Fülscher, P.-Å. Malmqvist, L. Serrano-Andrés, K. Pierloot, M. Merchán, *Adv. Chem. Phys.* **1996**, *93*, 219.
[49] L. Serrano-Andrés, R. Lindh, B. O. Roos, M. Merchán, *J. Phys. Chem.* **1993**, *97*, 9360.
[50] L. Serrano-Andrés, B. O. Roos, *J. Am. Chem. Soc.* **1996**, *118*, 185.
[51] O. Rubio-Pons, L. Serrano-Andrés, M. Merchán, *J. Phys. Chem. A* **2001**, *105*, 9664.
[52] Gaussian 98 (Revision A.7), M. J. Frisch, G. W. Trucks, H. B. Schlegel, G. E. Scuseria, M. A. Robb, J. R. Cheeseman, V. G. Zakrzewski, J. A. Montgomery, R. E. Stratmann, J. C. Burant, S. Dapprich, J. M. Millam, A. D. Daniels, K. N. Kudin, M. C. Strain, O. Farkas, J. Tomasi, V. Barone, M. Cossi, R. Cammi, B. Mennucci, C. Pomelli, C. Adamo, S. Clifford, J. Ochterski, G. A. Petersson, P. Y. Ayala, Q. Cui, K. Morokuma, D. K. Malick, A. D. Rabuck, K. Raghavachari, J. B. Foresman, J. Cioslowski, J. V. Ortiz, B. B. Stefanov, G. Liu, A. Liashenko, P. Piskorz, I. Komaromi, R. Gomperts, R. L. Martin, D. J. Fox, T. Keith, M. A. Al-Laham, C. Y. Peng, A. Nanayakkara, C. Gonzalez, M. Challacombe, P. M. W. Gill, B. G. Johnson, W. Chen, M. W. Wong, J. L.

Andres, M. Head-Gordon, E. S. Replogle, J. A. Pople, Gaussian, Inc., Pittsburgh, PA, **1998**..
[53] MOLCAS-5, 5.0 ed., K. Andersson, M. Baryz, A. Bernhardsson, M. R. A. Blomberg, P. Boussard, D. L. Cooper, T. Fleig, M. P. Fülscher, B. Hess, G. Karlström, R. Lindh, P.-Å. Malmqvist, P. Neogrády, J. Olsen, B. O. Roos, A. J. Sadlej, B. Schimmelpfennig, M. Schütz, L. Seijo, L. Serrano-Andrés, P. E. M. Siegbahn, J. Stålring, T. Thorsteinsson, V. Veryazov, U. Wahlgren, P.-O. Widmarw, Department of Theoretical Chemistry, Chemical Centre, University of Lund, P.O.B. 124, 22100 Lund, Sweden, **2000**.
[54] A. Bolovinos, P. Tsekeris, J. Philis, E. Pantos, G. Andritsopoulus, *J. Mol. Spectrosc.* **1984**, *103*, 240.
[55] G. Fischer, G. J. Small, *J. Chem. Phys.* **1972**, *56*, 5934.
[56] M. B. Robin, *Higher Excited States of Polyatomic Molecules*, *Vol.* 3, Academic Press, London, **1985**.
[57] H.-H. Perkampus, C. Schmiele, T. H. Braunschweig, *UV/Vis Atlas of Organic Compounds*, VCH, Weinheim, **1992**.
[58] S. J. Strickler, R. A. Berg, *J. Chem. Phys.* **1962**, *37*, 814.
[59] H. Saigusa, E. C. Lim, *J. Chem. Phys.* **1983**, *78*, 91.
[60] N. Ohta, O. Sekiguchi, H. Baba, *J. Chem. Phys.* **1988**, *88*, 68.
[61] D. A. Wiersma, *Chem. Phys. Lett.* **1972**, *16*, 517.
[62] P. U. d. Haag, W. L. Meerts, J. T. Hougen, *Chem. Phys. Lett.* **1991**, *151*, 371.
[63] A. E. W. Knight, C. S. Parmenter, *Chem. Phys. Lett.* **1979**, *43*, 257.
[64] M. Heaven, T. Sears, V. E. Bondybey, T. A. Miller, *J. Chem. Phys.* **1981**, *75*, 5271.
[65] M. Kasha, *Discuss. Faraday Soc.* **1950**, *9*, 14.
[66] N. Ohta, T. Takemura, *J. Phys. Chem. B* **1990**, *94*, 3466.
[67] D. J. Tozer, R. D. Amos, N. C. Handy, B. O. Roos, L. Serrano-Andrés, *Mol. Phys.* **1999**, *97*, 859.
[68] S. Fantacci, A. Migani, M. Olivucci, *J. Phys. Chem. A* **2004**, *108*, 1208.

Received: July 27, 2004
Revised: October 19, 2004